Construction and Building Materials 483 (2025) 141768

Contents lists available at ScienceDirect

Construction and Building Materials

journal homepage: www.elsevier.com/locate/conbuildmat

The influence of curing method on properties of laterite soil based geopolymer cement

Zeyneb kemal Nuru [a,*,1], Walied A. Elsaigh [a,2], Elsabe P. Kearsley [b,3]

[a] Department of Civil & Environmental Engineering and Building Science, University of South Africa, Johannesburg, South Africa
[b] Department of Civil Engineering, University of Pretoria, Pretoria, South Africa

ARTICLE INFO

Keywords:
Calcined Laterite soil
Geopolymer cement
Curing methods
Mechanical properties
Characterization

ABSTRACT

The paper investigates the effect of curing conditions on the properties of laterite soil-based geopolymer cement. In the experimental testing, calcined laterite soil was used as a solid precursor in the preparation of geopolymer cement. Standard size prismatic geopolymer specimens were prepared and subjected to four curing methods, including open air curing and courses of combined open-air curing and oven curing. The prisms were tested at 3, 7, and 28 days to determine the effect of curing methods on the flexural and compressive strengths. The crushed prisms were further pulverised and analysed to investigate the microstructure, elemental composition, mineralogical phases, chemical bonding, and thermal behaviour. The findings showed that the highest strength at 28 days was obtained with the air curing method. However, the curing methods involving an oven curing course resulted in the highest early strength at 3(early strength) and 7 days.

1. Introduction

The term "geopolymer" was coined in the 1970s by Davidovits to describe an alternative cementitious material obtained by combining alkali solution with reactive aluminosilicate materials through polycondensation process at temperatures below 100°C [1]. According to the review by Duxson et al. [2] the precursor materials utilised in the production of geopolymer cement need to be rich in both silicon (Si) and aluminum (Al). These materials can be sourced out either from geological deposits such as kaolinite clay, or from industrial by-products like fly ash, bottom ash, and slag.

In the past, precursors such as fly ash and other waste materials were used to produce geopolymer cements, however, due to unavailability in some geographical locations, there was a shift towards exploring naturally available materials. Recent studies reveal that geopolymer cement can be produced using laterite soil [3]. Lateritic soils are predominantly found in environments that have undergone leaching and oxidation, resulting in a distinct reddish or yellowish colour deposit. These soils are underlain by cemented gravels and laterite, which consist of goethite, hematite, quartz, and kaolinite [4]. Laterite soil is highly abundant in many African countries, including Ethiopia and South Africa [5–7].

Polycondensation process leads to the formation of dense structures in the form of gel-like material that has cementitious properties. According to Davidovits [1] the geopolymer gel (i.e., geopolymer cement paste) is made up of a chemical structure that is three-dimensional in nature, consisting of silico-poly sialate (-SiO-Al-O-), poly sialate-siloxo (Si-O-Al-O-Si-O), and apoly sialate-disiloxo (-Si-O-Al-O-Si-O-Si-O). In a later study involving laterite-based geopolymer gel, ferro-silico-aluminate (-Fe-O-Si-O-Al-O-) was identified as an additional compound in this three-dimensional structure [3].

To manufacture geopolymer cement from laterite soil, alkalis are used to activate the calcined soil powder. Tiffo et al. [8] and Mathew and Issac [9] found that the greatest geopolymer synthesis occurs with an alkali made by combining sodium silicate (Na_2SiO_3) and sodium hydroxide (NaOH) with a ratio in the range of 1–2.5, and a NaOH solution with a molarity range of 8–16 M. They further recommended that the combined alkali solution be left for a period of 24 hours in a sealed glass container to depolymerise at room temperature for 24 hours before using it. Kamseu et al. [10] in their investigation, utilized 8 M NaOH to activate calcined laterite soil, achieving an initial setting time of 2 hours. Moreover, the ideal fresh and hardened properties of geopolymer cement can be obtained by maintaining an alkali to solid (i.e., precursor)

* Correspondence to: UNISA Florida Campus, Johannesburg 1710, South Africa.
E-mail addresses: 17460069@mylife.unisa.ac.za (Z. Nuru), hussiwam@unisa.ac.za (W.A. Elsaigh), elsabe.kearsley@up.ac.za (E.P. Kearsley).
[1] ORCID; https://orcid.org/0009-0007-1111-4192
[2] ORCID; https://orcid.org/0000-0002-1668-3104
[3] ORCID: https://orcid.org/0000-0003-0458-8908

https://doi.org/10.1016/j.conbuildmat.2025.141768
Received 6 December 2024; Received in revised form 11 March 2025; Accepted 11 May 2025
Available online 17 May 2025

ratio between 0.5 and 0.65 [11–13].

Curing is crucial to the development of the polycondensation reaction and to maintaining the desired properties of geopolymer. Limited research exists on curing methods for geopolymer paste, mortar and concrete, often with conflicting and inconclusive results regarding the optimal curing method. Three primary curing methods are commonly used in the literature, including open air curing, oven curing, and steam curing. Tests on geopolymer cement paste utilising various precursor materials including low reactive volcanic ash [14] blend of fly ash and ground granulated blast furnace slag, GGBFS [15], and red mud-fly ash [16] revealed that polycondensation reaction is significantly enhanced by open air curing. In contrast, the investigation by Chouksey et al. [17] found that oven curing is more efficient as compared to open air curing when using a precursor by blending fly ash and GGBF. The investigation by Nadia et al. [18] found that laterite-based geopolymer samples cured in an oven have greater strength than those cured in open air, but the highest strength was observed in samples cured with steam.

The study by Sajan et al. [19] revealed that the uniaxial compressive strength of fly ash-based geopolymer increases by elevating the curing temperature from 20 to 60°C. The maximum strength was recorded at 36.21 MPa after 14 days of curing, while increasing the curing temperature to 80°C resulted in a reduction in strength to 32.26 MPa. In the study on red mud -based geopolymer by Singh et al. [16], the compressive strength of geopolymer reached 43.8 MPa for ambient curing conditions. Laterite-based geopolymer cured at 70 °C for 2 hours reached a compressive strength of 40 MPa [20]. The study by Kaze et al. [21] examined the potential of using calcined iron-rich aluminosilicate, specifically laterite soil, as a precursor for producing alkali-activated mortars. When cured at 80 °C, the material achieved compressive and flexural strengths of up to 32.2 MPa and 12.1 MPa, respectively, after 28 days. In the study by Nkwaju et al. [22], the compressive strength of the laterite-based geopolymer composite was reported to be 50 MPa, with a flexural strength of 6 MPa.

This paper aims to investigate the effect of four different curing methods on the properties of laterite-based geopolymer cement. The optimum curing methods was selected based on the analysis of the strength of replicate prisms specimens and other characterization techniques. The results suggest that the properties of a hardened geopolymer paste is greatly influenced by the curing methods, with open air curing appearing to be the most effective.

2. Materials and methods

2.1. Materials

2.1.1. Laterites soil

Raw laterites, reddish in colour, were collected from a road construction site located in Roodepoort, South Africa. The collected material was sieved to obtain particles smaller than 150 micrometres. Thereafter, the soil was subjected to calcination at a temperature of 700°C for a duration of 4 hours and left to cool down in the oven until soil reached room temperature. The chemical composition of the calcined powder was determined through X-ray fluorescence spectrometer testing. The main components of the calcined laterite soil are 66.23 % silicon dioxide (SiO_2), 20.72 % aluminum oxide (Al_2O_3), and 6.95 % iron oxide (Fe_2O_3), which make up approximately 93.9 % of its composition. According to ASTM C618–19 [23], This chemical makeup highlights the pozzolanic nature of laterite soil, making it a suitable precursor for the production of geopolymer cement.

2.1.2. Activator

A mixture of Na_2SiO_3 and 8 M NaOH in a mass ratio of 1:2.5 was used to make the alkali solution, which was then used to activate the calcined laterite for the geopolymer paste production. The 8 M sodium hydroxide solution was formulated by dissolving 99.45 % pure sodium hydroxide pellets in water. The activator solutions were mixed together and allowed to depolymerise for a period of 24 hours prior to being mixed with the calcined laterite.

2.2. Preparation of geopolymer cement paste

The geopolymer paste was prepared by mixing the calcined laterites with the alkali activator at a mass ratio of 1:0.65. A mechanical mixer, typically used for Portland cement mortar, was employed for 9 minutes to ensure a uniform mixture. The fresh geopolymer mixture was poured into standard metal prism moulds measuring 40 mm× 40 mm x 160 mm, and the surface was finished and immediately covered with plastic sheets to prevent moisture evaporation. All mix parameters were kept unchanged except the method of curing. Table 1 shows the specimens' designations and the courses involved in each curing method.

2.3. Methods

The sets of three prismatic specimens, each measuring 40 × 40 x 160 mm, underwent four different curing methods. The flexural strength of the geopolymer was tested at ages of 3, 7 and 28 days, and the mean value was calculated for each age. The two six broken prims (i.e., prisms' halves) were further tested to determine the compressive strength at the same ages. The hardened geopolymer prisms tested at 28 days were pulverised and characterised using Scanning Electron Microscopy (SEM), Energy-Dispersive X-ray Spectroscopy (EDS), X-ray diffraction (XRD), Fourier Transform Infrared (FTIR), Thermogravimetric Analysis (TGA), Differential Thermal Analysis (DTA), and pH. XRD analysis was performed using a Malvern Panalytical Aeris diffractometer equipped with a PIXcel detector and fixed slits, utilizing Fe-filtered Co-Kα radiation. Phase identification of the geopolymer powder samples and calcined laterite was conducted using the X'Pert HighScore Plus software, in conjunction with the PAN-ICSD database, over a 2θ range of 5–90 degrees. The JCM-6000PLUS Benchtop SEM, coupled with an Oxford EDS were used to establish the microstructural properties. Prior to FTIR and TGA analysis, the ground geopolymer samples were stored in a desiccator. FTIR analysis was performed using a Bruker VERTEX FTIR Spectrometer equipped with a diamond ATR fitting, was employed to identify the main chemical groups. The results were recorded within a wave range between 400 cm^{-1} and 4000 cm^{-1}.TGA and DTA measurements were performed simultaneously. The measurements were performed by increasing the temperature from 30 °C and 1200 °C at a rate of 5 °C per minute under a nitrogen purge. The pH was typically determined by dissolving the powder samples in deionized water at a ratio of 1:5 (solid to solvent).

Table 1
Curing method designation and description.

Specimens Designation	Description
ACL	The moulds were filled with geopolymer cement paste and left at room temperature for a period of 24 hours, specimens were demoulded, covered with plastic, and left at room temperature until tested.
OCL24	The moulds were filled with geopolymer paste, covered with plastic, and left at room temperature for a period of 24 hours. The specimens were demoulded and placed in the oven at 65 °C for a period of 24 hours; thereafter, the specimens were taken out of oven and left at room temperature until tested.
OCL2	The moulds were filled with geopolymer paste, covered with plastic, and left at room temperature for a period of 2 hours before they were placed in the oven at 65 °C for a period of 24 hours. The specimens were demoulded and left at room temperature until tested.
IOCL	The moulds were filled with geopolymer paste and immediately placed in oven at 65°C for a period of 24 hours. The specimens were demoulded and left at room temperature until tested.

3. Results and discussion

3.1. Strength properties of hardened geopolymer paste

The flexural strength values and their corresponding standard deviations (SD) for the four curing sequences are shown in Table 2. Additionally, the strength development at curing ages of 3, 7, and 28 days is illustrated in Fig. 1. The samples placed in the oven 24 hours after casting (OCL24) achieved the highest flexural strength. In contrast, immediate heating (IOCL) led to the lowest strength at 7 and 28 days. This indicates that the geopolymer produced from calcined laterite soil exhibits brittle behaviour, a trait typical of ceramic-like microstructures, particularly when subjected to immediate oven curing. This finding is supported by the XRD analysis, which suggests that the presence of crystalline quartz minerals may play a role in the material's brittleness. Specifically, the increased levels of crystalline quartz in OCL2 and IOCL correlate with a decrease in flexural strength.

The average compressive strength results illustrated in Fig. 2 show the prism specimens subjected to four different curing methods (i.e., ACL, OCL24, OCL2, and IOCL). The highest compressive strength recorded at 28 days was 51.5 MPa, exceeding the previously reported maximum strength of 32.2 MPa for geopolymer produced from alkali-activated laterite [24].

3.1.1. The effects of curing methods

The curing method has a significant impact on the compressive and flexural strength of geopolymers made from laterite soil. Notably, open air curing (ACL) achieved a compressive strength of 51.5 MPa, outperforming oven curing methods, which recorded strengths of 45.9 MPa for OCL24, 32.75 MPa for OCL2, and 26.93 MPa for IOCL, all measured at 28 days. This is consistent with findings from Singh et al. [16], which indicate that geopolymers produced using fly ash and red mud demonstrate the highest strength when subjected to heat curing. However, this contrasts with the findings of Sajan et al. [19], who observed that geopolymer specimens cured at 20°C in open air exhibited lower strength than those cured in an oven at 60°C. Furthermore, Kaze et al. [24], indicated that compressive strength increases with curing temperatures between 20 and 80°C.

3.1.2. The effects of curing age

The results indicate the age effect on the strength of ACL and the impact of a 24-hour open-air curing period applied immediately after casting and before oven curing (see OCL24 description in Table 1). Notably, the compressive strength increased significantly from 21.9 MPa to 51.5 MPa between 3 and 28 days, representing a 57.5 % increase in strength. This finding aligns with the study by Sajan et al. [19], which reported that the compressive strength of the geopolymer increased from 6 to 24 MPa over the same period, resulting in a 75 % increase. In contrast, Fig. 2. illustrate the samples subjected to oven curing showed no significant strength development relative to curing age. This lack of improvement may indicate that the geopolymerisation process was completed within the first 24 hours in the oven, and no further strength development occurred as curing age increased.

The results indicate that ACL curing is favorable, as it achieves the highest strength after a longer curing duration of 28 days. In addition to strength, ACL offers advantages over oven curing methods in terms of energy consumption and aligns well with conventional curing practices for in situ construction. Oven curing combined with 24 hours of open-air curing also yields competitive results compared to ACL. Therefore, this finding suggests that the geopolymerisation process requires adequate time to develop a strong matrix structure. Furthermore, it concludes that oven curing at 60°C for 24 hours is sufficient to reach maximum strength without needing an extended curing period.

Table 2
Flexural Strength and Standard Deviation of Geopolymer Paste.

Sample ID	3 Days (MPa)	SD (MPa)	7 Days (MPa)	SD (MPa)	28 Days (MPa)	SD (MPa)
ACL	2.74	0.22	3.57	0.77	5.25	0.77
OCL24	5.81	0.63	6.48	0.24	5.82	0.53
OCL2	4.76	0.33	5.50	0.88	5.40	0.25
IOCL	3.76	0.18	3.97	0.33	4.01	0.62

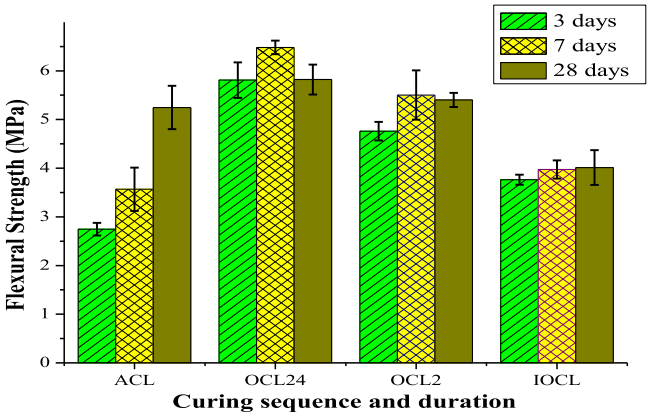

Fig. 1. Flexural strength of synthesised geopolymer with four curing methods.

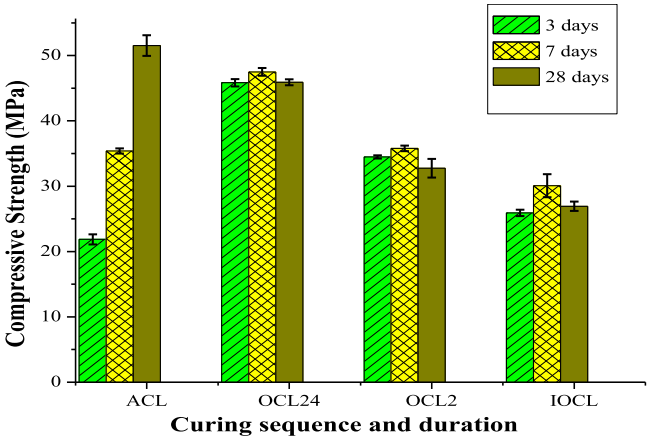

Fig. 2. Compressive strength of synthesized geopolymer with four curing methods.

3.2. Bulk density of hardened geopolymer

The bulk density values of the four resulting geopolymers are presented in Fig. 3. The bulk density of sample ACL varies with curing age, decreasing as the age increases. This reduction in bulk density observed in the ACL samples can be attributed to their absorption of water from the mix and the evaporation of moisture from the structure, leading to a decrease in density. However, at 28 days of curing, ACL exhibits a density almost similar to that of the other samples (OCL24, OCL2, and IOCL). In contrast, the bulk densities of samples OCL2 and IOCL show a slight increase with age, which may be due to moisture absorption through the cracks and void surface from the environment. According to Kaze et al. [24], the higher bulk density of laterite-based geopolymers corresponds to a lower number of voids in the matrix, resulting from the formation of the geopolymer structure. However, this paper indicates that a higher bulk density is associated with reduced flexural and compressive strength. This suggests that geopolymer products require sufficient time to complete the geopolymerisation process, allowing for a stable bulk density or the evaporation of moisture within the structure, particularly when air curing is employed, which may relate to the

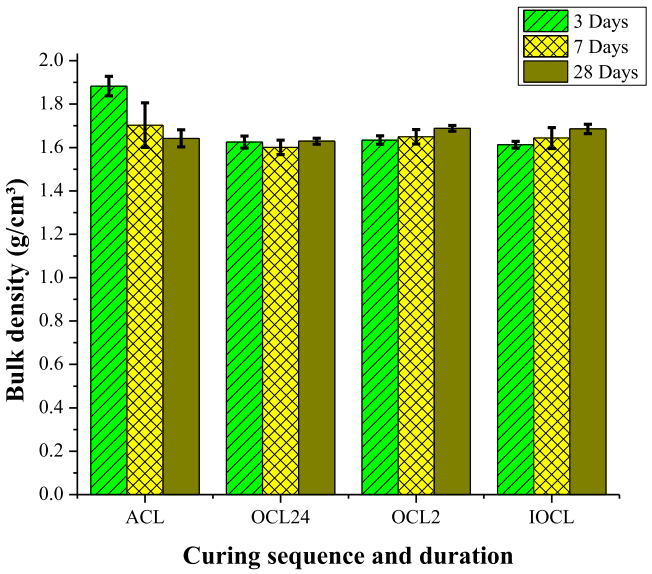

Fig. 3. Bulk density of synthesized geopolymer with four curing methods.

findings of the strength presented in this paper.

3.3. Characterization of hardened geopolymer paste

3.3.1. SEM and EDS Analyses

Fig. 4 presents SEM images illustrating the morphological structure of hardened geopolymer paste that was exposed to different curing methods (i.e., ACL, OCL24, OCL2, and IOCL).

The SEM images of geopolymer ACL, shown in Fig. 4a, reveal a few pores and microcracks in noncritical zones (inside pores). The cracks do not extend significantly because the pores are surrounded by a dense structure. A similar trend is observed in Fig. 4b, for the OCL24 sample, indicating a higher formation of the geopolymer product, which is supported by EDS analysis showing that the matrix consists of N-A-F-S-H gel. The microstructures of ACL and OCL24 align well with the strength findings and further demonstrate that oven curing, after a relatively long open curing period (≥ 24 hours), is as effective as open-air curing.

In Fig. 4c, the OCL2 sample displays a structure characterized by sheet-like shapes, pores, and microcracks. According to Fekoua [18], the presence of these sheet-like shapes is related to the presence of non-reactive minerals. This study also suggests that the formation of these sheet-like structures indicates a high presence of unreacted or crystalline quartz, as confirmed by the XRD analysis. When connecting this result to the strength test, the cracks seen in the SEM image seem to stem from incomplete geopolymer matrix formation. This may suggest insufficient polymerization or weak bonding within the structure. Meanwhile, Fig. 4d for IOCL displays a less homogeneous structure with poor cohesion between particles, an uneven surface, and microcracks. This lack of cohesion, along with semi-reacted particles and cracks, may be attributed to water evaporation during oven curing before sufficient formation of the geopolymer matrix. The reduced formation of the geopolymer matrix in this structure results in low strength, which aligns with the strength findings. This underscores the importance of allowing sufficient open-air curing time for laterite-based geopolymer to achieve proper adhesion of the constituent minerals before undergoing temperature exposure during oven curing.

Fig. 5 shows the elemental composition of ACL and IOCL, presented

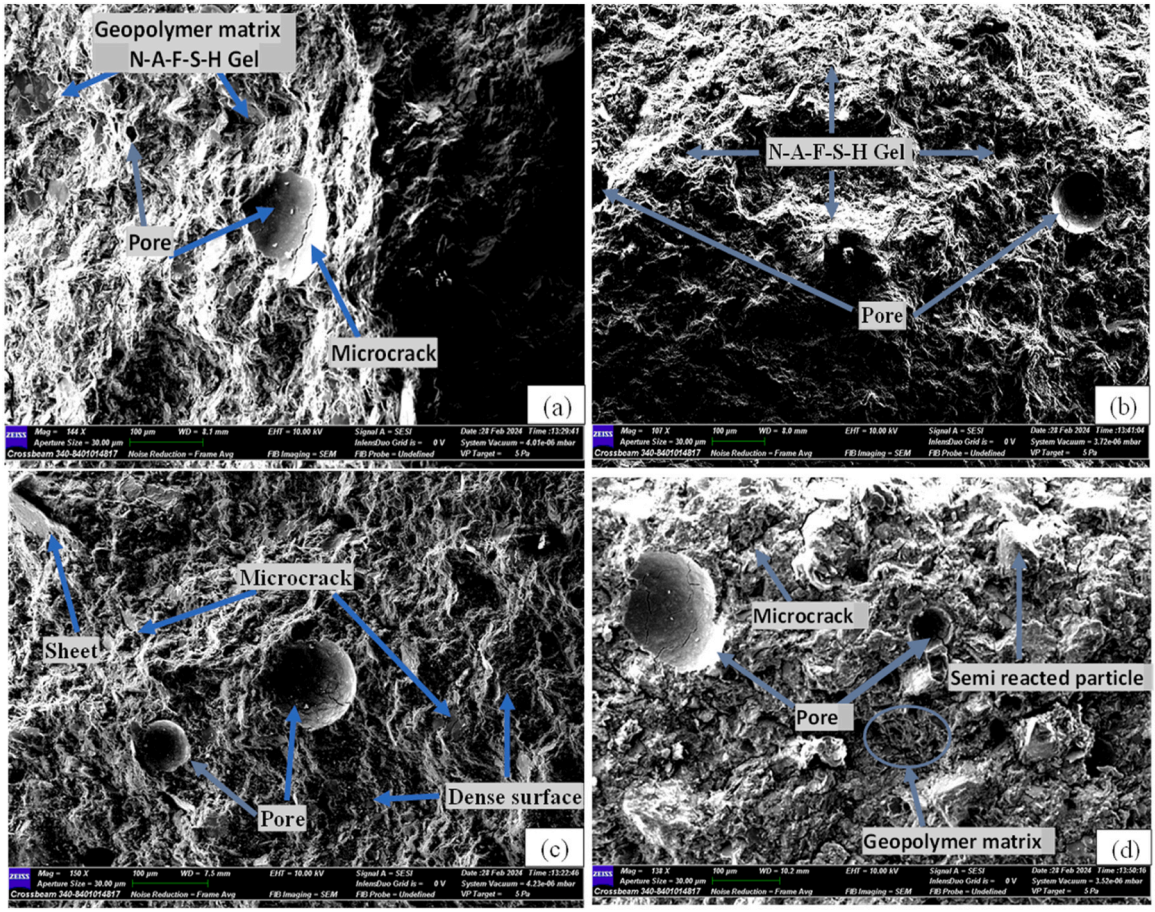

Fig. 4. SEM image with four curing methods (a) ACL (b), OCL24 (c), OCL2 (d) IOCL.

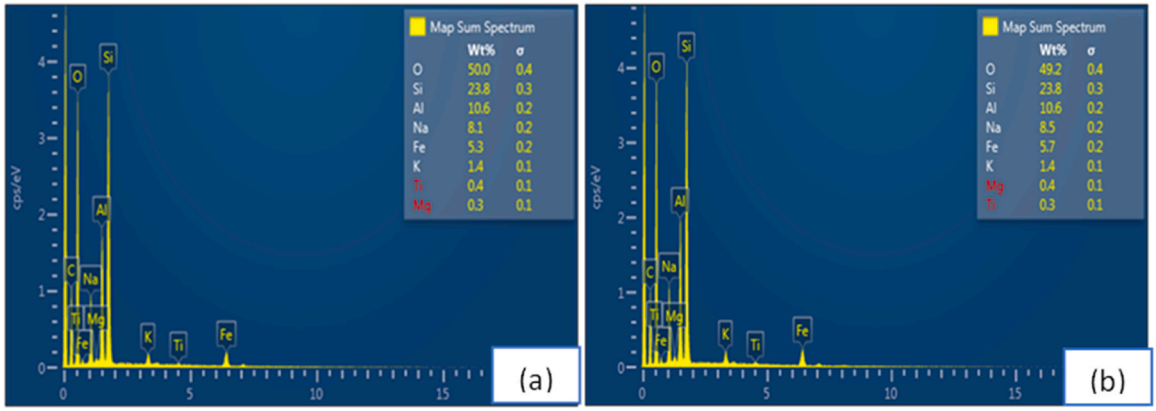

Fig. 5. EDS analysis (a) ACL, (b) IOCL.

in 5(a) and 5(b), respectively. The EDS results indicate that the two different curing method did not change the quantities of the primary elements (O, Si, Al, Na, and k) present in the geopolymer matrix. The EDS maps for each of these primary elements are available but are not presented due to size limitations. However, the maps indicate an even distribution over the geopolymer matrix, suggesting uniform bonding structure. It is important to note that the presence of these elements indicates that the geopolymers matrix is composed of N-A-F-S-H gel and other networks including Si–O–Al–O–Fe, Al–O–Fe, Si–O–Fe, and Si–O–Si. The formation of these chemical compounds was also confirmed by the IFTR, which is presented in a later section of this paper.

3.3.2. *XRD analysis*

The detection limit of the XRD instrument ranges from 0.5 to 3 wt percent, meaning that some minerals below this threshold cannot be presented in the table. Table 3 shows that the primary mineral components of the calcined laterite soil include quartz ($Si_1\ O_2$), muscovite ($H_{1.828}\ Al_{2.472}\ F_{0.172}\ Fe_{0.315}\ K_1\ O_{11.828}\ Si_{3.28}$), hematite ($Fe_2O_3$), microcline ($Al_1\ K_1\ O_8\ Si_3$) and biotite ($H_{2.548}\ Al_{2.432}\ Fe_{2.427}\ K_{1.891}\ Mg_{3.09}\ Mn_{0.035}\ Na_{0.062}\ O_{24}\ Si_{5.568}\ Ti_{0.448}$), with a low amount of albite ($Al_1\ Na_1\ O8\ Si_3$). The primary mineral composition was consistently observed across all curing methods (ACL, OCL24, OCL2, and IOCL), although the quantities of each mineral varied. Notably, the amount of quartz in the geopolymer sample is higher than in the laterite due to the presence of an alkali activator, which increases the silica content. This finding aligns with the EDS results, indicating a high silica content that is reflected in the XRD results as increased quartz levels.

Microcline was detected in small quantities in the OCL24 sample and in trace amounts (below the detection limit) in the ACL sample, while it was absent in the other two samples. Albite, although present in undetectable amounts in laterite, was completely absent in all four geopolymer samples, suggesting its dissolution during the reaction process. Additionally, anatase (O_2Ti_1) emerged as a newly formed mineral phase in the activated products of both curing methods (ACL and OCL24) but was not detected in the precursor material. However, XRF analysis confirmed the presence of this oxide. The inability to detect anatase in the laterite sample may be due to the limited sample size analyzed and may not fully represent its overall distribution.

Fig. 6 displays the crystalline materials that are present in the

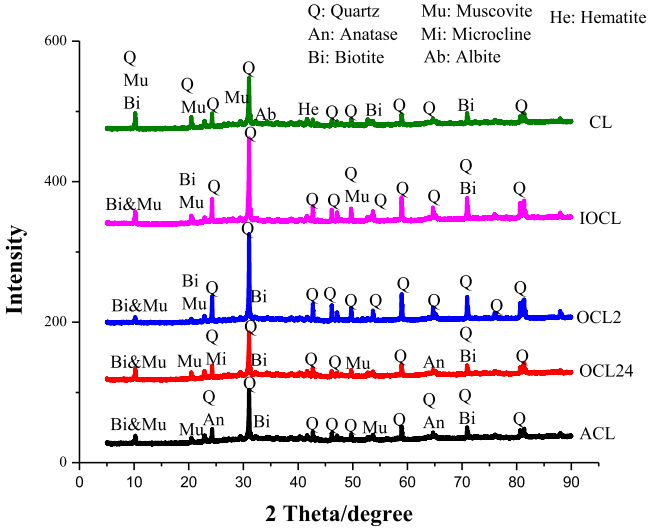

Fig. 6. XRD analysis results.

samples. A high-intensity peak is recorded between 30 and 35 degrees, corresponding to quartz, particularly in samples OCL2 and IOCL. A small peak of hematite was observed in laterite; however, it disappears in the geopolymer due to its transformation into an amorphous phase. Although the amounts of anatase and biotite are below the detectable limit, the figure indicates they are in a crystalline phase. The crystalline minerals observed in the precursor soil have only partially transformed into the hardened geopolymer paste, indicating that they are not fully dissolved in the alkali activator. According to Poudeu et al. [25], the undissolved crystalline minerals serve as fillers in the geopolymer product. Furthermore, low peak intensities were observed in the geopolymer product. Kaze et al. [26] suggest that this behavior indicates that the respective minerals in the precursor soil have transformed from a crystalline to an amorphous form, becoming reactive. When comparing the four curing methods, lower intensities were associated with ACL and OCL24.

Table 3
Mineralogical composition of geopolymer paste.

	Quartz	Anatase	Biotite	Muscovite	Microcline	Albite	Hematite
CL	49.9	-	5.5	24.9	9	0.0	10.7
ACL	64.9	1.5	3.6	19.9	0.0	-	5.6
OCL24	59.7	1.1	10.5	22.9	2.7	-	3.1
OCL2	84.9	0.6	0.0	13.2	-	-	1.3
IOCL	83.1	0.7	3.8	11	-	-	1.3

The quartz content increased significantly in OCL2 and IOCL, while muscovite, hematite, and biotite showed a marked reduction, and microcline was completely absent. Additionally, these two samples exhibited higher peak intensity compared to ACL and OCL24, indicating the presence of more crystalline minerals. The reduction or disappearance of certain minerals, along with the higher peak intensity, suggests a slowdown in geopolymerisation reactions, ultimately leading to a decrease in strength.

3.3.3. FTIR Analyses

The FTIR transmittance spectra of laterite-based geopolymer cement for the four curing methods used in this study are presented in Fig. 7.

Concerning IOCL and OCL2 samples, peaks were observed in the range 3663 cm^{-1} to 2351 cm^{-1}, and a band observed at 1647 cm^{-1}. According to both Lecomte-Nana et al. [27], and Bewa et al. [28] peaks in the range 3663 cm^{-1} to 2351 cm^{-1} indicate the presence of stretching vibrations of O-H while the band at 1647 cm^{-1} is attributed to bending vibration of H–O–H. The latter expresses surfaces that absorbed or entrapped water in large cavities of the geopolymer network. The absorption of water in the synthesised sample causes strength reduction. In addition, a band is observed at 1384 cm^{-1} in IOCL. According to Abbas et al. [29], this band is associated with the stretching vibration of the O-C-O bond, a consequence of carbonation in geopolymers.

In the four tested samples, the main band is observed at approximately 984 cm^{-1} in the FTIR spectra. According to Kaze et al. [30] this broad band is an indication- of the formation of asymmetric and symmetric stretching of the Si-O-T bonds, with the (T) representing Si, Al, or Fe. Furthermore, this band is indicative of the geopolymer gel structure, meaning all curing methods have led to formation of geopolymers, but to different degrees.

A weak band at 680 cm^{-1} and the last wavenumber at 585 cm^{-1} were observed. As stated by Panias et al. [31], these peaks relate to a symmetric stretching vibration of the Si-O-Al and Si-O-Si groups, associated with geopolymers.

The bands from 3663 cm^{-1} to 1647 cm^{-1} were not observed in ACL and OCL24, suggesting the absence of O-H in the geopolymer. The disappearance of the band1384 cm^{-1} is also indicating the absence of efflorescence (i.e., carbonation). Furthermore, the peak at 779 cm^{-1} in ACL is attributed to the symmetric stretching vibration of Si-O-Si as suggested by Panias et al. [31]. In general, the absence of the O-H and efflorescence relates to an increased degree of geopolymerisation, which may explain the higher strengths obtained for ACL and OCL24.

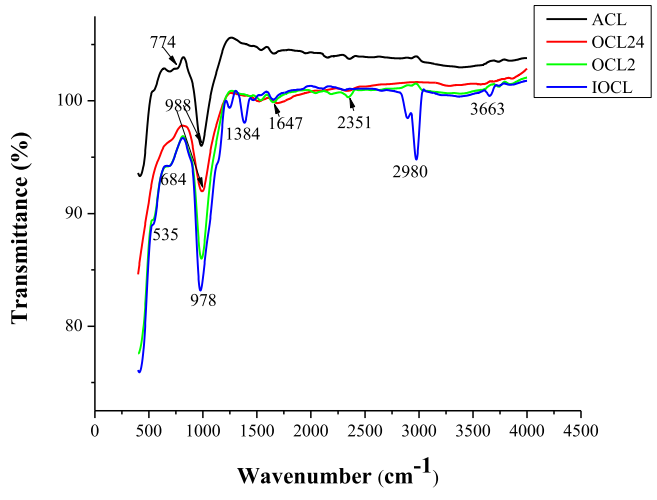

Fig. 7. FTIR spectra of laterite soil based geopolymer syntesized using four curing sequnces.

3.3.4. TGA and DTA analysis

The thermal stability of hardened geopolymers pastes were analysed by using TGA and DTA. Fig. 8 shows the thermogravimetric curves of ACL, OCL24, OCL2, and IOCL cured samples. The observed mass loss during heat treatment of the geopolymers is likely due to water evaporation and dihydroxylation effects.

Three regions relating to temperature ranges can be identified from the TGA and TDA curves. These are region I, region II, and region III corresponding to temperature ranges of 20–120 °C, 120–300 °C and > 300 °C, respectively. Region I, relates to the loss of hygroscopic (free) water, while region II indicates the evaporation of chemically bonded water from the hardened geopolymers' structure. Region III is characterised by the evaporation of the hydroxyl groups and the decomposition of chemical bonds essential to the geopolymer structure, such as Si-O-Al, Si-O-Fe, and Si-O-Si [2,32–34].

Concerning the DTA curve for the ACL sample, endothermic peaks were observed in region I. In OCL2 and OCL24 samples, the endothermic peak was observed in region II. Nergis et al. [35] suggest this behaviour is indicative of water loss during the formation of the geopolymer gel. However, in the IOCL sample, endothermic peaks were observed in all regions, showing an overlap in the removal of hygroscopic and crystalline water. The endothermic and exothermic peaks are associated with the decomposition of compounds, indicating a loss of the geopolymer matrix.

The TGA curves indicate that the mass loss in region III for ACL, OCL24, OCL2 and IOCL samples ranges is between 1.6 % and 2.8 %, with more than 80 % of the occurs in region II. Above 700 °C all samples showed a negligible mass loss of approximately 0.35 %. It is worth pointing out that the total mass loss of all synthesised geopolymer samples falls between 10 % and 12 %. Interestingly, the ACL sample, which did not undergo temperature curing during synthesis, exhibited the lowest rate of mass loss across all three regions. This observation may be attributed to the fact that ACL geopolymer is more stable. On the other hand, the immediate oven cured geopolymer sample (IOCL) showed lower stability due to the decomposition of chemical compounds, as observed in the DTA graph. This analysis, supported by SEM imaging, revealed weak formation of the geopolymer matrix. XRD analysis showed minimal transformation of crystalline phases into an amorphous structure, FTIR analysis indicates the O-H bond presented and strength tests confirmed a lower development of compressive and flexural strength.

3.3.5. pH analysis

The pH values of the ACL, OCL24, OCL2, and IOCL cured samples were 10.30, 10.27, 10.40, and 10.25, respectively. The four curing techniques do not appear to influence pH values. The pH value of the precursor soil was measured as 5.66. Comparing the pH values of the precursor and the cured samples indicate that laterite soil with 8 M NaOH improved alkalinity by about 63 % (ie., from 5.66 to above 10). This is in line with the study by Anburuvel [36], who found that geopolymerisation happens when the pH range is between 10 and 13. In the study by Saride and Jallu [37] the fly ash precursor had a pH ranging from 8 to 11, while the geopolymer cement made from fly ash and NaOH with concentrations ranging from 0.5 to 6 M yielded a final pH of 13. This suggests that the low pH value of precursor materials requires a high concentration of alkali activators to achieve desired pH range (10−13) necessary for the geopolymerisation to take place.

4. Conclusions

The conclusions drawn from this study are as follows:

1. ACL and OCL24 resulted in the highest compressive and flexural strength growth as compared to OCL2 and IOCL. The laterite-based geopolymer requires sufficient time before undergoing any temperature changes to achieve the improved mechanical strength and

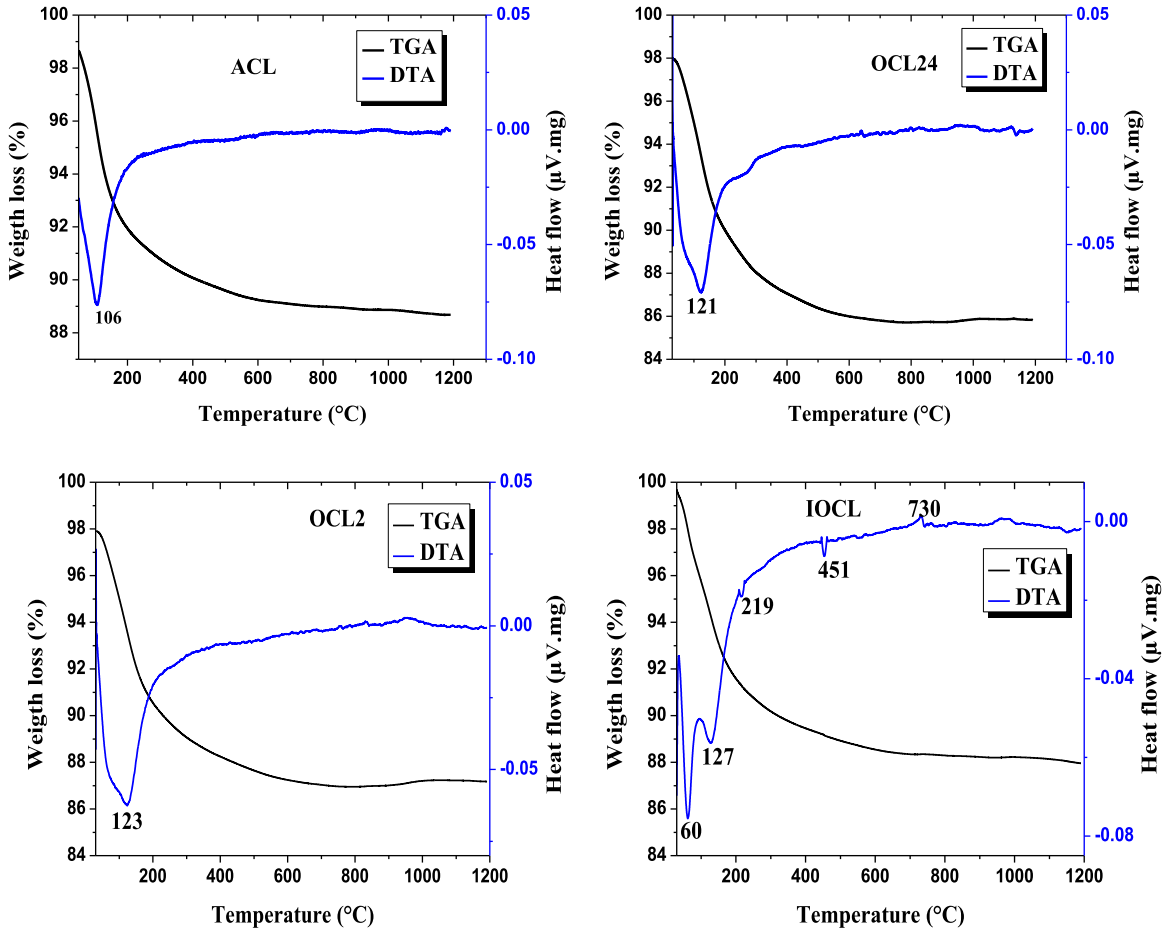

Fig. 8. TGA and DTA curves of geopolymer cement for four curing methods.

thermal stability. Most of the strength development occurs within the initial 24 hours when the oven curing course is applied, with minimal to no strength increase as the curing time progresses. Conversely, there is a consistent increase in strength as the curing age increases up to 28 days. OCL24 provides an ideal curing method for situations where there is a need for high early strength.

2. The microstructure of hardened geopolymer cement paste following ACL and OCL24 revealed a dense and compact behaviour methods, indicating good interfacial bonding between the particles. The reduced strength with no or short open curing duration before the oven curing duration is due to less bonding and a less dense structure.
3. The XRD analysis indicates a decrease in crystallinity, suggesting that the four curing methods improve mineral dissolution within the alkali activator, with remaining minerals serving as fillers, particularly noticeable in the ACL and OCL24 curing methods. This effect is attributed to the lack of large voids that would otherwise trap water within the geopolymer structure. This observation is consistent with the EDS results, which show a high concentration of silica and oxygen. Furthermore, the FTIR spectra show a wide wavelength band and the loss of OH groups, which confirms the formation of the geopolymer.
4. The thermal behaviour of the ACL, OCL24, OCL2, and IOCL curing methods showed mass loss of 1.6–2.8 % due to the decomposition of hydrated phases (at temperatures $\geq$ 300° C) and a considerable mass loss of about 80 % occurred at temperatures in the range 120–300°C. However, the main chemical bond of geopolymer decomposition is observed in IOCL in DTA analysis. These analyses indicated that the ACL, OCL24, and OCL2 exhibited stable behaviour as compared to IOCL. Geopolymerisation occurs when the pH of the activated precursor is greater than 10. Laterite precursor has a relatively low pH, which will require an alkali activator with high concentration.

Funding

The University of South Africa provides the scholarship and covers the cost of required materials.

CRediT authorship contribution statement

Walied A. Elsaigh: Writing – review & editing, Visualization, Validation, Supervision, Investigation, Formal analysis. **Nuru Zeyneb Kemal:** Writing – review & editing, Methodology, Investigation, Formal analysis, Data curation, Conceptualization. **Elsabe P. Kearsley:** Writing – review & editing, Validation, Supervision, Formal analysis.

Declaration of Competing Interest

The authors declare that they have no known competing financial interests or personal relationships that could have appeared to influence the work reported in this paper.

Acknowledgements

The author would like to thank the laboratory personnel of the department of Civil Engineering, department of Chemistry Science, and the Institute for Nanotechnology and Water Sustainability (iNanoWS) at Unisa for their support in conducting the experimental work reported in

this paper.

Data Availability

Data will be made available on request.

References

[1] J. Davidovits, Geopolymers: inorganic polymeric new materials, J. Therm. Anal. Calor. 37 (8) (1991) 1633–1656, https://doi.org/10.1007/bf01912193.

[2] P. Duxson, C. Chemicals, S. National, J. Provis, Geopolymer technology: the current state of the art, Geopolymer Technol.: Curr. State Art. (2007), https://doi.org/10.1007/s10853-006-0637-z.

[3] J. Davidovits, R. Davidovits, Ferro-sialate Geopolymers (-Fe-O-Si-O-Al-O-), (2020). https://doi.org/10.13140/RG.2.2.25792.89608/2.

[4] I. Kheoruenromne, Red and Yellow Soils And Laterite Formation In The Northeast Plateau, Thailand, 1987.

[5] W.J. Morin, P.C. Todor, R. De, J. Brazil Dner, Laterite and Lateritic soils and other problem soils of the tropics. Instructional Manual, II, Agency for International Development, Washington, DC, 1975.

[6] A. Teklay, M. Haile, A. Teferra, E.J. Murray, The effect of sample preparation and testing procedure on the geotechnical properties of tropically weathered residual laterite soils of Ethiopia, Zede J. 33 (2015) 45–62.

[7] D.M. Helgren, K.W. Butzer, Paleosols of the southern Cape Coast, South Africa: implications for laterite definition, genesis, and age, Geogr. Rev. (1977) 430–445.

[8] E. Tiffo, J. Batiste, B. Mbah, D. Placide, J. Noel, Y. Djobo, A. Elimbi, Physical and mechanical properties of unheated and heated kaolin based-geopolymers with partial replacement of aluminium hydroxide, 239 (2020). https://doi.org/10.1016/j.matchemphys.2019.122103.

[9] G. Mathew, B.M. Issac, Effect of molarity of sodium hydroxide on the aluminosilicate content in laterite aggregate of laterised geopolymer concrete, J. Build. Eng. (2020) 101486, https://doi.org/10.1016/j.jobe.2020.101486.

[10] E. Kamseu, C.R. Kaze, J.N.N. Fekoua, U.C. Melo, S. Rossignol, C. Leonelli, Ferrisilicates formation during the geopolymerization of natural Fe-rich aluminosilicate precursors, Mater. Chem. Phys. 240 (2020), https://doi.org/10.1016/j.matchemphys.2019.122062.

[11] J. Valdès, S. Metekong, C.R. Kaze, A. Adesina, J. Giogetti, D. Nemaleu, J. Noel, Y. Djobo, P. Ninla, L. Thamer, Influence of Thermal Activation and Silica Modulus on the Properties of Clayey-Lateritic Based Geopolymer Binders Cured at Room Temperature, Silicon (2022) 7399–7416, https://doi.org/10.1007/s12633-021-01566-7.

[12] C.R. Kaze, P. Ninla Lemougna, T. Alomayri, H. Assaedi, A. Adesina, S. Kumar Das, G.L. Lecomte-Nana, E. Kamseu, U. Chinje Melo, C. Leonelli, Characterization and performance evaluation of laterite based geopolymer binder cured at different temperatures, Constr. Build. Mater. 270 (2021) 121443, https://doi.org/10.1016/j.conbuildmat.2020.121443.

[13] C.R. Kaze, L.M. Beleuk à Moungam, M. Cannio, R. Rosa, E. Kamseu, U.C. Melo, C. Leonelli, Microstructure and engineering properties of Fe2O3(FeO)-Al2O3-SiO2 based geopolymer composites, J. Clean. Prod. 199 (2018) 849–859, https://doi.org/10.1016/j.jclepro.2018.07.171.

[14] J. Baenla, I.B.D. Li, B.D.M. Priso, P.D.B. Belibi, J.B.B. Mbah, A. Elimbi, Effects of curing regimes on mechanical strength and durability of alkali-activated low reactive volcanic ashes, Mater. Chem. Phys. 311 (2024) 128533, https://doi.org/10.1016/j.matchemphys.2023.128533.

[15] M.N.S. Hadi, H. Zhang, S. Parkinson, Optimum mix design of geopolymer pastes and concretes cured in ambient condition based on compressive strength, setting time and workability, J. Build. Eng. (2019) 301–313, https://doi.org/10.1016/j.jobe.2019.02.006.

[16] S. Singh, M.Uddappa Aswath, R.V. Ranganath, Effect of mechanical activation of red mud on the strength of geopolymer binder, Constr. Build. Mater. 177 (2018) 91–101.

[17] A. Chouksey, M. Verma, N. Dev, I. Rahman, K. Upreti, An investigation on the effect of curing conditions on the mechanical and microstructural properties of the geopolymer concrete, Mater. Res Express 9 (2022), https://doi.org/10.1088/2053-1591/ac6be0.

[18] J. Nadia, N. Fekoua, C.R. Kaze, L.L. Duna, A. Gharzouni, I.M. Ndassa, E. Kamseu, C. Leonelli, J. Nadia, N. Fekoua, C.R. Kaze, L.L. Duna, A. Gharzouni, Effects of curing cycles on developing strength and microstructure of goethite-rich aluminosilicate (corroded laterite) based geopolymer composites, Mater. Chem. Phys. 270 (2023) 124864.

[19] P. Sajan, Tengyao Jiang, ChooiKim Lau, Gang Tan, Kam Ng, Combined effect of curing temperature, curing period and alkaline, Clean. Mater. 1 (1921), https://doi.org/10.1016/j.clema.2021.100002.

[20] Subaer, A. Haris, A. Irhamsyah, N. Akifah, N.S. Amalia, Physico-Mechanical Properties of Geopolymer Based on Laterite Deposit Sidrap, South Sulawesi, in: J Phys Conf Ser, Institute of Physics Publishing, 2019, https://doi.org/10.1088/1742-6596/1244/1/012037.

[21] C.R. Kaze, S. Tome, G.L. Lecomte-Nana, A. Adesina, H. Essaedi, S.K. Das, T. Alomayri, E. Kamseu, U.C. Melo, Development of alkali-activated composites from calcined iron-rich laterite soil, Mater. (Oxf.) 15 (2021), https://doi.org/10.1016/j.mtla.2021.101032.

[22] R.Y. Nkwaju, J.N.Y. Djobo, J.N.F. Nouping, P.W.M. Huisken, J.G.N. Deutou, L. Courard, Iron-rich laterite-bagasse fibers based geopolymer composite: Mechanical, durability and insulating properties, Appl. Clay Sci. 183 (2019) 105333, https://doi.org/10.1016/j.clay.2019.105333.

[23] ASTM C618-19, Standard Specification for Coal Fly Ash and Raw or Calcined Natural Pozzolan for Use in Concrete, ASTM International, 2019, https://doi.org/10.1520/C0618-1.

[24] C.R. Kaze, P.N. Lemougna, T. Alomayri, H. Assaedi, A. Adesina, S. Kumar Das, G. L. Lecomte-Nana, K. Elie, U.C. Melo, L. Cristina, Characterization and performance evaluation of laterite based geopolymer binder cured at different temperatures, Constr. Build. Mater. 270 (2021) 121443, https://doi.org/10.1016/j.conbuildmat.2020.121443.

[25] R.C. Poudeu, C.J. Ekani, C.N. Djangang, P. Blanchart, Role of heat-treated laterite on the strengthening of geopolymer designed with laterite as solid precursor, Ann. De. Chim.: Sci. Des. Mater. 43 (2019) 359–367, https://doi.org/10.18280/acsm.430601.

[26] C.R. Kaze, J.N.Y. Djobo, A. Nana, H.K. Tchakoute, E. Kamseu, C. Leonelli, H. Rahier, Effect of silicate modulus on the setting, mechanical strength and microstructure of iron-rich aluminosilicate (laterite) based-geopolymer cured at room temperature, Ceram. Int 17 (2018) 21442–21450, https://doi.org/10.1016/j.ceramint.2018.08.205.

[27] G. Lecomte-Nana, H. Goure-Doubi, A. Smith, A. Wattiaux, G. Lecomte, Effect of iron phase on the strengthening of lateritic-based “geomimetic” materials, Appl. Clay Sci. 70 (2012) 14–21, https://doi.org/10.1016/j.clay.2012.09.014.

[28] C.N. Bewa, H.K. Tchakouté, C.H. Rüscher, E. Kamseu, C. Leonelli, Influence of the curing temperature on the properties of poly(phospho-ferro-siloxo) networks from laterite, SN Appl. Sci. 1 (2019), https://doi.org/10.1007/s42452-019-0975-5.

[29] R. Abbas, M.A. Abdelzaher, N. Shehata, M.A. Tantawy, Production, characterization and performance of green geopolymer modified with industrial by - products, Nat. Publ. Group UK (2024), https://doi.org/10.1038/s41598-024-55494-8.

[30] C.R. Kaze, L.M. Beleuk, M.L.F. Djouka, A. Nana, E. Kamseu, U.F.C. Melo, C. Leonelli, The corrosion of kaolinite by iron minerals and the effects on geopolymerization, Appl. Clay Sci. 138 (2017) 48–62, https://doi.org/10.1016/j.clay.2016.12.040.

[31] D. Panias, I.P. Giannopoulou, T. Perraki, Effect of synthesis parameters on the mechanical properties of fly ash-based geopolymers, Colloids Surf. A: Physicochem. Eng. Asp. 301 (2007) 246–254, https://doi.org/10.1016/j.colsurfa.2006.12.064.

[32] R. He, N. Dai, Z. Wang, Thermal and mechanical properties of geopolymers exposed to high temperature: a literature review, Adv. Civ. Eng. 2020 (2020), https://doi.org/10.1155/2020/7532703.

[33] M.D.M. Paiva, E.C.C.M. Silvab, D.M.A. Melo, A.E. Martinellid, J.F. Schneidere, A geopolymer cementing system for oil wells subject to steam injection, J. Pet. Sci. Eng. 169 (2018) 748–759, https://doi.org/10.1016/j.petrol.2018.06.022.

[34] P. Rico, A. Adriano, G. Soriano, J. Duque, Fifth International symposium on energy characterization of water absorption and desorption properties of natural zeolites in ecuador, in: Fifth International Symposiym on Energy, Puerto Rico Energy Center-Laccei, 2013, pp. 1–9.

[35] D.D.B. Nergis, M.M.A.B. Abdullah, A.V. Sandu, P. Vizureanu, XRD and TG-DTA Study of new alkali activated materials based on fly ash with sand and glass powder, Materials 13 (2020) 343, https://doi.org/10.3390/ma13020343.

[36] A. Anburuvel, The role of activators in geopolymer-based stabilization for road construction: a state-of-the-art review, Multiscale Multidiscip. Model., Exp. Des. 6 (2023) 41–59, https://doi.org/10.1007/s41939-022-00139-4.

[37] S. Saride, M. Jallu, Effect of Fly Ash Geopolymer on Layer Coefficients of Reclaimed Asphalt Pavement Bases, J. Transp. Eng., Part B: Pavements 146 (2020) 04020033, https://doi.org/10.1061/jpeodx.0000169.